Available online at www.sciencedirect.com
SCIENCE DIRECT®
Applied Catalysis A: General 283 (2005) 99–109
APPLIED CATALYSIS A: GENERAL
www.elsevier.com/locate/apcata

Kinetics of the homogeneous hydrogenation of avermectins catalyzed by $RhCl(Ph_3P)_3$ complexes

Patricia D. Zgolicz[1], María I. Cabrera[2], Ricardo J. Grau*[,2]

INTEC (Instituto de Desarrollo Tecnológico para la Industria Química, Universidad Nacional del Litoral (UNL) and Consejo Nacional de Investigaciones Científicas y Técnicas (CONICET)), Güemes 3450, 3000 Santa Fe, Argentina

Received 6 August 2004; received in revised form 29 December 2004; accepted 29 December 2004
Available online 1 February 2005

Abstract

The kinetics of the hydrogenation of avermectins B_{1a} and B_{1b} catalyzed by $RhCl(Ph_3P)_3$ complexes was studied in a temperature range of 298–328 K at 275.7 kN m^{-2}, using catalyst loading in the range of 0.75–7.25 wt.% with respect to the avermectins in toluene solution. The effects on the hydrogenation rate of the catalyst, avermectins, and hydrogen concentrations were determined under complete induction time suppression and without catalyst deactivation. Rate equations were developed for various kinetic schemes on the basis of the main steps suggested by Wilkinson for simple olefin hydrogenation and fitted to the experimental data. A statistical analysis of regression using three plausible mechanisms of reaction allows a discussion on the adequacy of the models to approach the observed half-order reaction with respect to the catalyst loading and first-order to avermectins and hydrogen concentrations. A reaction mechanism featuring non-extensive simple dissociation of the catalyst precursor and reaction pathway along the hydride route with the rate-determining olefin coordination step proved fair enough to describe the hydrogenation of this macrocyclic lactone. The physical reasonability of the equilibrium and kinetic parameters was also discussed.
© 2005 Elsevier B.V. All rights reserved.

Keywords: Avermectins; Hydrogenation; Wilkinson catalyst; Rhodium complexes; Kinetic modeling

1. Introduction

Avermectins are macrocyclic lactones with potent anthelmintic and anti-parasitic activity produced by fermentation of *Streptomyces avermitilis*. By biotechnological techniques known to those skilled in the art, the actinomycete yields four homologous pairs of closely related macrolides, which are further subdivided into major components A_{1a}, A_{2a}, B_{1a} and B_{2a}, and minor components A_{1b}, A_{2b}, B_{1b} and B_{2b}. A generalized structure of these avermectins is shown in Fig. 1. Avermectins B_{1a} and B_{1b} provide the basis for more bioactive semi-synthetic 22,23-dihydro analogues, which compose the active components of commercial ivermectin [1]. This potent anthelmintic and ectoparasiticide agent is widely used in animal health.

The process for preparing ivermectin involves the regiospecific reduction of the olefinic linkage between carbons 22 and 23 of avermectins B_{1a} and B_{1b}, without affecting the remaining four double bonds. Because the target olefin is the only cis substituted and sterically the least hindered of the five double-bonds, the Rh(I) complex $[RhCl(Ph_3P)_3]$, often called Wilkinson's catalyst [2], is typically used for this purpose [1,3]. Amounts of this catalyst in the 0.05–0.5 mol/mol of avermectin range are employed to achieve <98% yields of ivermectin. Because of the high cost of rhodium, further attempts have been made to reduce these considerable amounts of catalyst, and to improve the recovery process for removing and recycling the catalyst, have been made but without significant improvements. Rhodium complexes, which in addition to phosphines, also contain hydrazines as ligands are suitable to carry out the hydrogenation using lower catalyst charges [4]. However,

* Corresponding author. Tel.: +54 342 4511539; fax: +54 342 4511597.
E-mail address: cqfina@ceride.gov.ar (R.J. Grau).
[1] Research Assistant from CONICET.
[2] Professor at UNL and Member of CONICET's Research Staff.

0926-860X/$ – see front matter © 2005 Elsevier B.V. All rights reserved.
doi:10.1016/j.apcata.2004.12.040

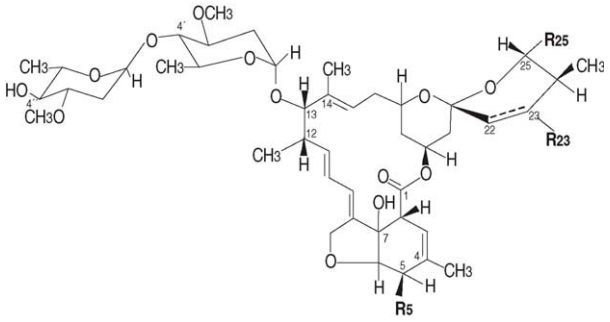

Avermectins	R_5	R_{23}	R_{25}	22,23 bond
A_{1a} (+)	$-OCH_3$	−H	sec-butyl	double
A_{1b}	$-OCH_3$	−H	iso-propyl	double
A_{2a} (+)	$-OCH_3$	−OH	sec-butyl	single
A_{2b}	$-OCH_3$	−OH	iso-propyl	single
B_{1a} (+)(++)	−OH	−H	sec-butyl	double
B_{1b} (++)	−OH	−H	iso-propyl	double
B_{2a} (+)	−OH	−OH	sec-butyl	single
B_{2b}	−OH	−OH	iso-propyl	single

(+) Major component.
(++) By selective reduction of the 22,23 bond yields ivermectin

Fig. 1. Generalized structure of avermectins.

too high reaction times are still observed under the most demanding reaction conditions. Rhodium complexes having the formula $[RhCl(R_3P)_3]$, where R is an alkyl-substituted phenyl group, are easier to be recovered from the homogeneous reaction medium due to the lipophilic properties of this type of phosphines [5]. Rhodium complexes prepared in situ with sulphonated aryl-substituted phosphines, are useful to carry out the avermectin hydrogenation in organic and aqueous-organic reaction media [6]. Even though the heterogeneous system appears to be convenient for recycling the catalyst, too high rhodium charges are certainly required. Therefore, over 20 years later the process developed by Chabala is still widely used.

To improve the avermectin hydrogenation process on the basis of the reaction engineering, the kinetic information, if any, is scant. Until now the mechanism of reaction is not entirely clear and the kinetics has not been studied specifically. This lack of basic information prompted us to carry out an extensive kinetic study of the homogeneous hydrogenation before exploring the heterogeneous systems as an alternative route to avoid the disadvantages related to the recovery of the unsupported complexes. This first contribution is primarily concerned with the kinetic modeling of the homogeneous hydrogenation of avermectins catalyzed by chlorotris(triphenylphosphine) rhodium(I) $RhCl(Ph_3P)_3$. Special care has been taken to remove impurities from the commercial avermectins to avoid undesirable effects caused by poisoning of the catalyst and to work at lower catalyst loading. After interpretation of the hydrogenation rate data in a wide range of operating conditions, the analysis focuses on the kinetic modeling in order to throw some light on the reaction mechanism governing the selective hydrogenation of avermectins B_{1a} and B_{1b} to ivermectin. A statistical analysis of regression based on three plausible mechanisms of reaction allows a discussion on the adequacy of the model that best fits our experimental data. The underlying reaction steps of the Wilkinson's model for the hydrogenation of simple olefins provide the basic framework from which to derive the rate equations. However, the half-order dependence on the catalyst concentration observed in the whole range of the catalyst loading is ascribed to a non-extensive simple dissociation of the catalyst precursor and not to some dimerisation of the Wilkinson's catalyst at higher concentrations, or to a concentration-dependent change from one active catalytic species to a less active one, as suggested earlier for the hydrogenation of other olefins with Rh complexes.

2. Experimental

2.1. Catalyst and chemicals

Chlorotris(triphenylphosphine) rhodium(I) catalyst (Aldrich, 99.99%) was used in the hydrogenation experiments. Avermectin B_1 (purity > 98.75%; B_{1a} > 94.5% and B_{1b} > 4.25%) was obtained by purification of commercially available avermectin (Over, 95%) as described below. Toluene (Cicarelli, puriss. p.a.) was used as received. Nitrogen gas (AgaGas, 99.999% pure) and hydrogen gas (AgaGas, 99.999% pure) were flowed through a Deoxo unit and a drying column before use. Hydrogenation experiments were performed using purified avermectin unless otherwise stated.

2.2. Apparatus and operating conditions

The experimental setup is schematically shown in Fig. 2. All hydrogenation experiments were performed isothermally in a 300 mL pressurized semibatch reactor (Parr Instruments Co., Model 4842) equipped with a feeder reservoir and a cup-and-cap device for substrate and catalyst preconditioning, respectively. The reactor temperature was controlled within ±0.5 K by electrical heating and a heat exchanger attached to the coolant circulation system to achieve a fast dynamic control. The pressure was measured with a strain-gauge pressure transducer (Ashcroft, Model K2) and maintained within ±10 kN m^{-2} with a pressure controller (Cole Parmer, Model 68502-10). The stirring velocity was settled with a variable-speed impeller provided by the manufacturer of the reactor system. Hydrogen flow was monitored with a mass flow meter (Matheson 8110).

The kinetic experiments were carried out in the 298–328 K range and at 275.7 kN m^{-2} of hydrogen pressure. The catalyst loading was in the range of 0.75–7.25 wt.% with respect to avermectin. A stirring rate of 250 rpm was sufficient to ensure that the gas–liquid resistance for

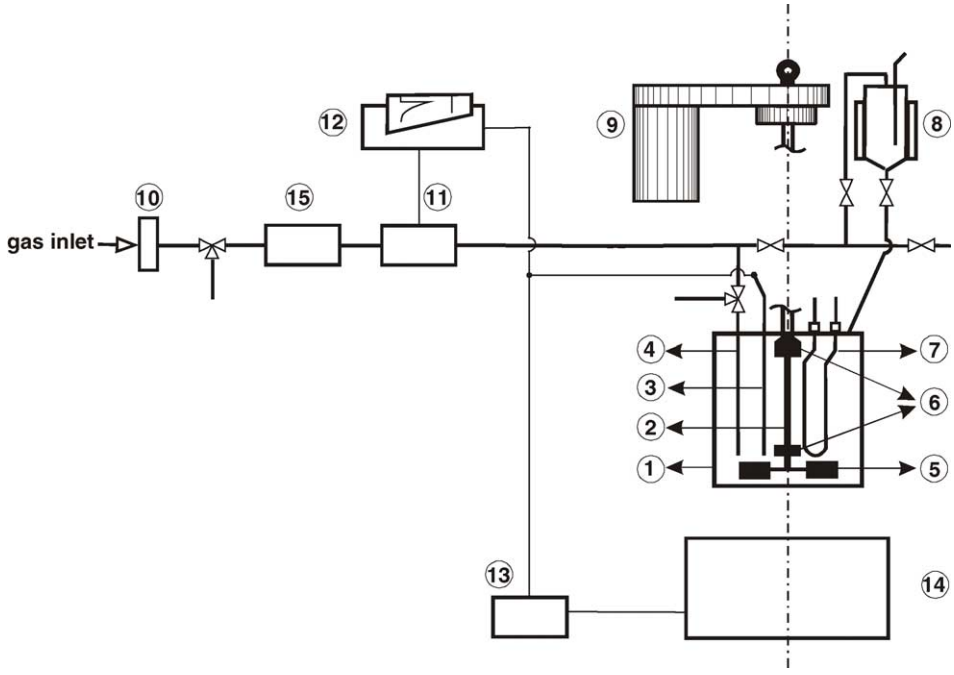

Fig. 2. Experimental setup: (1) reaction vessel; (2) shaft stirrer; (3) temperature sensor; (4) sampling valve; (5) impeller; (6) CAC device; (7) cooling coil; (8) feeder reservoir; (9) stirrer motor; (10) pressure controller; (11) mass flow meter; (12) chart recorder; (13) temperature controller; (14) electrical heating furnace; (15) electronic pressure transducer.

hydrogen transfer be negligible, as experimentally corroborated by varying the impeller speed up to 750 rpm. Indicative values of the gas–liquid mass transfer resistance were obtained according to the technique reported in Appendix A. Only a few experimental data are moderately affected by the gas absorption resistance. They correspond to the initial step of the hydrogenation run carried out under the most demanding conditions (catalyst loading of 7.25 wt.%, at 323 K). However, this undesirable effect is practically negligible in all other hydrogenation runs because the maximum values of the relative concentration drop of the hydrogen at the gas–liquid interface were found to be less than 3.8%. Therefore, at the stirring rate applied and with the reactor configuration used, the liquid phase is almost fully saturated with hydrogen.

Since the kinetic study demands zero induction times, reproducibility and constant level of catalytic activity, the feeder reservoir and cup-and-cap device were useful to fulfil all these requirements as described in the experimental procedure. The reproducibility of experimental data was excellent.

2.3. Experimental procedure

Induction and poisoning effects were observed when the commercial avermectin was used as received, and the hydrogenation technique was as described in the literature [3]. These effects were apparent from the examination of both concentrations versus time and initial rate versus catalyst loading profiles. A substantial qualitative and quantitative improvement was obtained developing a new procedure: the avermectin was purified prior to use as detailed below, and the substrate and toluene solution of $RhCl(Ph_3P)_3$ were in situ preconditioned to avoid induction effects due to slow catalyst dissolution and/or hydrogen saturation, and/or in situ activation of the catalyst during the beginning period. In addition, the procedure allowed a simpler handling and contacting of reagents. The improvements are shown in Fig. 3.

A typical procedure was as follows: toluene (90 mL) was charged into the reactor vessel, and a precise amount of catalyst was placed in the cup mounted on the upper part of the cup-and-cap device according to the technique previously reported [7]. The reactor was assembled, and then degassed by mild vacuum, purged three times with nitrogen and flushed with hydrogen at room temperature. Under hydrogen atmosphere, the catalyst was embedded into the toluene by a sudden stop of the mechanical stirring. While the catalyst dissolves in the toluene solution, the reactor was pressurized with hydrogen and heated up to the reaction conditions. On the other hand, a toluene solution of purified avermectin (30 mL, 10.35 wt.%) was charged into the feeder reservoir and then degassed, pressurized and saturated with hydrogen at the reaction temperature following a procedure similar to that described for the conditioning of the toluene solution of catalyst. Once the reaction conditions were stabilized, the reaction was allowed to start by the simple opening of the connecting valve between the pressurized feeder reservoir and the reaction vessel. Zero time was taken just at that moment because the reagents and catalyst came into intimate contact almost instantaneously by effect of the intense agitation. Induction

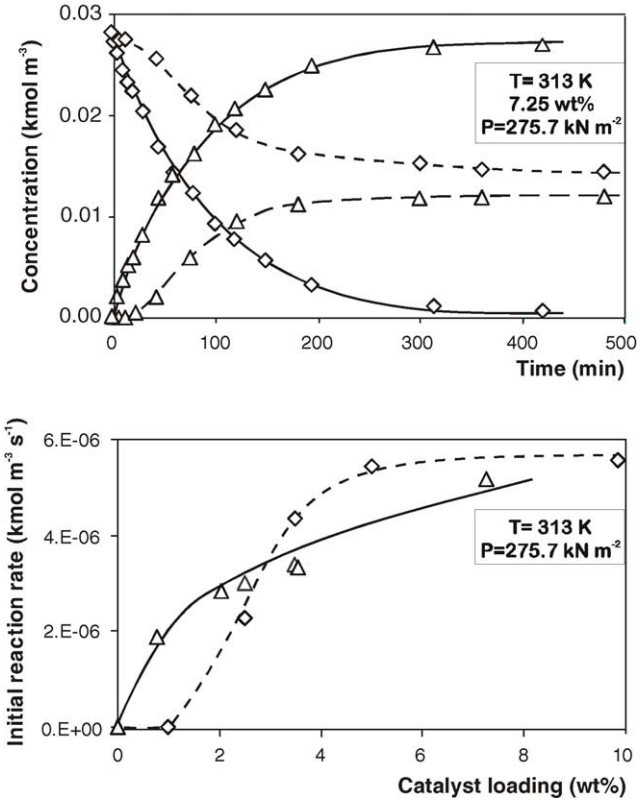

Fig. 3. Typical concentration vs. time, and initial reaction rate vs. catalyst loading curves without (dotted-line) and with (full-line) both purification of avermectins and special devices (feeder reservoir and CAC device). (◇) avermectin; (Δ) ivermectin.

and poisoning effects were not observed in any of the experiments. Samples of the reaction mixture were withdrawn at different time intervals and analyzed by HPLC. The reaction was stopped as soon as no detectable avermectin consumption occurred.

2.4. Analytical method

The liquid samples were analyzed using a HPLC system with resolution of avermectin analogues and hydrogenated derivatives thereof. The analyses were performed on a liquid chromatograph (Shimadzu LTO-10A/LC-10AS) equipped with a diode-array detector (Shimadzu SPD-M10A), using a C18 column (Nucleosil C18, 150 mm × 4.6 mm i.d., 5 μm) under the following conditions: acetonitrile/methanol/water (56:26:16) as mobile phase; flow rate: 1 mL/min; detection: UV, 246 nm; temperature: 303 K.

2.5. Purification of the avermectin

A toluene solution of avermectin (30 mL, 6.5 wt.%) was added to an aqueous solution of NaOH (15 mL, 10 wt.%). The immiscible solutions were stirred for 2 h at 323 K, and then left to stand until complete separation of the phases. After removing the alkaline aqueous phase, the organic-phase was washed repeatedly with water. An ulterior washing with controlled addition of acetic acid until neutralization afforded the toluene solution of avermectin to be justly hydrogenated.

3. Results and discussion

3.1. Effect of the catalyst loading

To determine the dependence of the hydrogenation rate on the catalyst concentration, a series of experiments was carried out by varying the catalyst loading from 0.75 to 7.25 wt.% at each temperature (298, 313 and 328 K) and keeping constant the hydrogen pressure (275.7 kN m^{-2}). Results are shown in Fig. 4a–b. The hydrogenation rate versus catalyst loading plots display a break around 1 wt.%, from which the observed higher dependence at low concentration decreases significantly with increasing catalyst loading, as shown in Fig. 4a. This feature has been attributed to some dimerisation of the Wilkinson's catalyst at higher concentrations [2], or to a concentration-dependent change from one active catalytic species to a less active one, as suggested for $RhH(CO)(PPh_3)_3$ and $RhCl(PPh_3)_3$ [8,9]. Accordingly, the dissociative pathway of the catalyst precursor $[RhCl(PPh_3)_3]$ (AP) in toluene solution (S) could be composed of a first dissociation yielding the solvated species $[RhCl(PPh_3)_2(S)]$ (AS), with subsequent secondary dimerisation into species $[RhCl(PPh_3)_2]_2$ $(A)_2$ or further dissociation to give species $[RhCl(PPh_3)(S)_2]$ (AS_2). Based on these arguments, it could be speculated that the observed behavior is due to the prevailing formation of (AS_2) and $(A)_2$ species at low and high catalyst concentrations, respectively. However, for the same experimental data, we found that the hydrogenation rate approaches a half-order dependence on the catalyst concentration in the whole range of the catalyst loading, as shown by the straight lines depicted in Fig. 4b. From this finding, we suggested that a more consistent explanation lies in the non-extensive simple dissociation of the catalyst precursor, which leads to the observed half-order dependence as discussed below.

3.2. Effect of the avermectin concentration

The hydrogenation rates for different substrate concentrations in the range of 0.50–2.95 × 10^{-2} kmol m^{-3} were calculated from the slope of the corresponding avermectin concentration versus time curves at each temperature (298, 313 and 328 K), keeping constant the hydrogen pressure (275.7 kN m^{-2}) and the catalyst loading (2.05 and 7.25 wt.%). The reciprocals of these rates were plotted against the reciprocal of substrate concentration in Fig. 5. The plots are straight lines with small positive ordinate. The observed linearity is in agreement with previous findings for hydrogenation of smaller olefins with the Wilkinson catalyst, and is consistent with a predominant pathway by

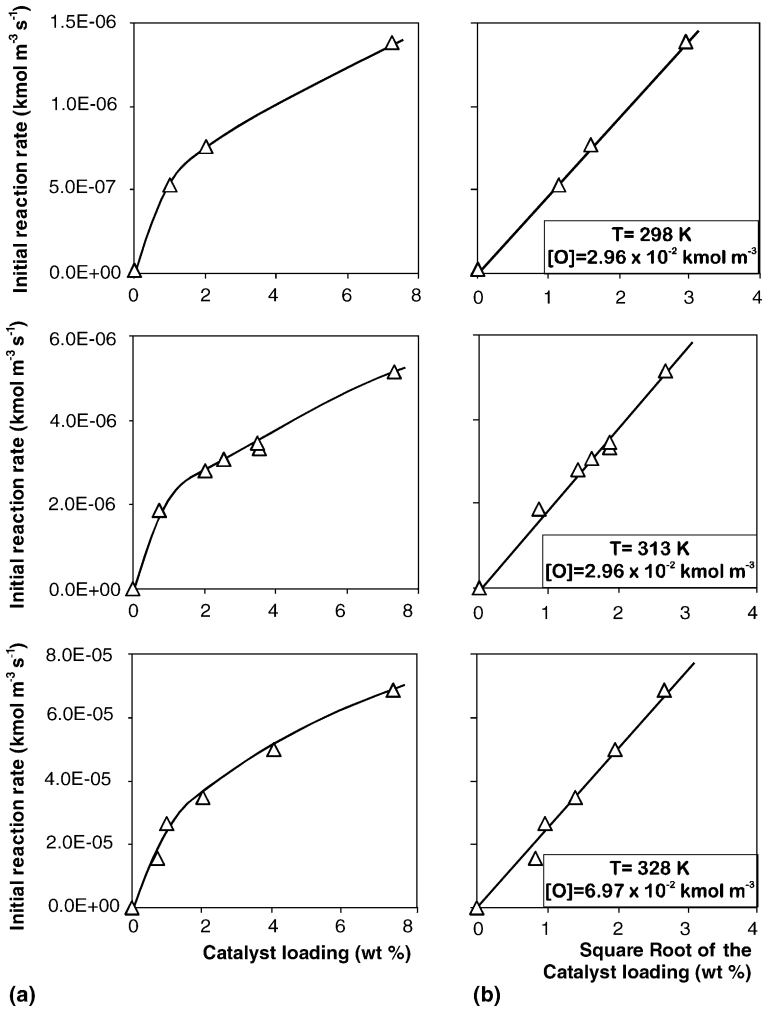

Fig. 4. Dependence of the hydrogenation rate on the catalyst concentration ranging from 0.75 to 7.25 wt.% at each temperature (298, 313 and 328 K), keeping constant the hydrogen pressure (275.7 kN m^{-2}). (a) First-order, and (b) half-order.

hydride route on the olefin route, as generally accepted for triphenylphosphine [10].

3.3. Effect of the hydrogen concentration

To analyze the dependence of the hydrogenation rate on the hydrogen pressure, a series of experiments was carried out by varying the hydrogen pressure over the range of 124.1–427.4 kN m^{-2} at each temperature (298, 313 and 328 K), keeping constant both the initial substrate concentration (2.96 × 10^{-2} kmol m^{-3}) and the catalyst loading (7.25 wt.%). The concentration of hydrogen dissolved in the reaction medium was calculated based on the hydrogen solubility in toluene [11]. Plots of the reciprocal of the

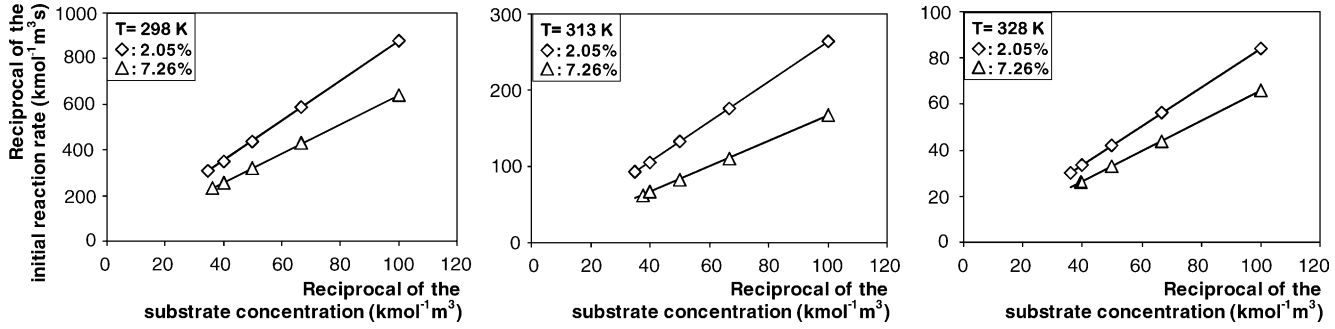

Fig. 5. Dependence of the hydrogenation rate on the avermectin concentration in the 0.50–2.95 × 10^{-2} kmol m^{-3} range, at each temperature (298, 313 and 328 K) and different catalyst loading (2.05 and 7.25 wt.%), keeping constant the hydrogen pressure (275.7 kN m^{-2}).

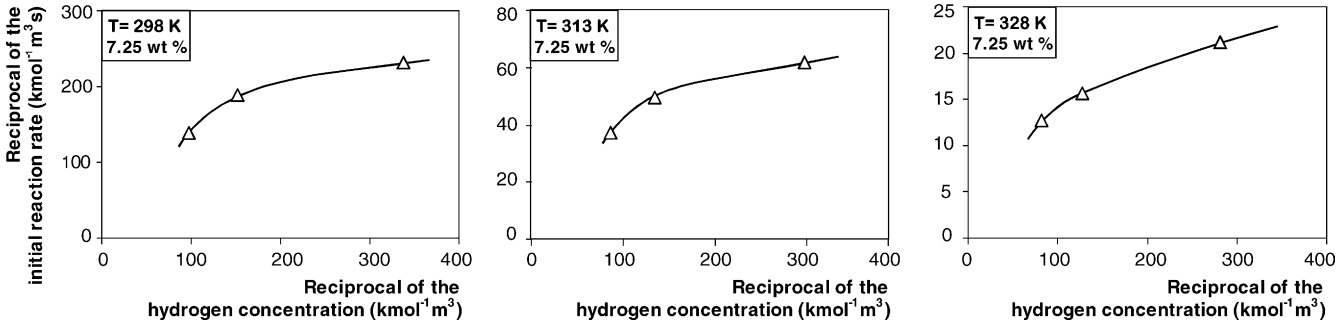

Fig. 6. Dependence of the hydrogenation rate on the hydrogen pressure over the range of 124.1–427.4 kN m^{-2} at each temperature (298, 313 and 328 K), keeping constant both the initial substrate concentration (2.96×10^{-2} kmol m^{-3}) and the catalyst loading (7.25 wt.%).

hydrogenation rate against the reciprocal of the concentration of dissolved hydrogen are decidedly non-linear, as shown in Fig. 6. These results demonstrate that the hydrogenation rate is lower than pseudo-first order with respect to the hydrogen concentration, which is also consistent with the prevailing hydride route.

3.4. Reaction mechanism and rate equations

The reaction mechanism involves the main equilibrium and elementary reaction steps suggested by Wilkinson to simple olefin hydrogenation [2], which also support evidence concerning the main features of the hydrogenation of this macrocyclic lactone. Many other schemes could be considered, e.g., direct dimerisation of the catalyst, hydrogenation of species AP followed by dissociation to species $RhCl(PPh_3)_3H_2(S)$, secondary deactivation pathways, etc. Several of their more complex model variants were indeed fitted. Because these models have more adjustable parameters but do not render deeper insight into the reaction mechanism, only the simplest ones were further pursued. They are designated as models M1–M3.

Kinetic model assumptions are as follows: (1) the equilibria are supposed to be reached fast, which implies that the quasi-equilibrium hypothesis is applicable for these steps; (2) the olefin coordination step is assumed to be rate-determining; (3) the rhodium and phosphines total concentrations are assumed to be constants.

3.4.1. Derivation of model M1

The simplest plausible model is taken as reference model, namely model M1. This model contains the physical assumptions underlying the kinetic model early proposed by Wilkinson and coworkers [2]. The reaction mechanism can be summarized according to the following scheme:

$$AS + H_2 \leftrightarrow ASH_2 \quad K_1(k_1 \text{and} k_{-1}) \tag{1}$$

$$AS + O_a \leftrightarrow ASO_a \quad K_{2a}(k_{2a} \text{and} k_{-2a}) \tag{2}$$

$$AS + O_b \leftrightarrow ASO_b \quad K_{2b}(k_{2b} \text{and} k_{-2b}) \tag{3}$$

$$ASH_2 + O_a \rightarrow AS + P_a \quad k_{3a} \tag{4}$$

$$ASH_2 + O_b \rightarrow AS + P_b \quad k_{3b} \tag{5}$$

$$ASO_a + H_2 \rightarrow AS + P_a \quad k_{4a} \tag{6}$$

$$ASO_b + H_2 \rightarrow AS + P_b \quad k_{4b} \tag{7}$$

where O_a and O_b represent the substrates (avermectins B_{1a} and B_{1b}) to be hydrogenated; P_a and P_b the hydrogenated derivatives (ivermectins). It should be noted that the hypothesis of complete dissociation of the catalyst precursor AP into AS underlies this mechanism.

The hydrogenation rate equations become:

$$R_a = k_{3a}K_1(1 + \hat{k}_{4a}\hat{K}_{2a})[H_2][AS][O_a] \tag{8}$$

$$R_b = k_{3b}K_1(1 + \hat{k}_{4b}\hat{K}_{2b})[H_2][AS][O_b] \tag{9}$$

in conjunction with the following algebraic equation arising from a balance on species having rhodium

$$[AS] \times \{1 + K_1[H_2] + K_{2a}[O_a] + K_{2b}[O_b]\} - [Rh]_T = 0 \tag{10}$$

where $\hat{k}_{4a} = k_{4a}/k_{3a}$, $\hat{K}_{2a} = K_{2a}/K_1$, $\hat{k}_{4b} = k_{4b}/k_{3b}$ and $\hat{K}_{2b} = K_{2b}/K_1$. The kinetic and equilibrium constants remain to be found as adjustable parameters.

3.4.2. Derivation of model M2

In this variant it is additionally assumed that the dissociation of the catalyst precursor AP to AS takes place sparingly in the presence of toluene solution of avermectins. Therefore, the following elementary step for the dissociation of AP into AS is added to the reaction mechanism described by Eqs. (1)–(7):

$$AP + S \leftrightarrow AS + L \quad K_0(k_0 \text{and} k_{-0}) \tag{11}$$

where L represents phosphine ligand. Solving the rhodium and phosphine balances for AS gives:

$$[AS]\left\{1 + \frac{[AS]}{K_0}\right\} \times \{1 + K_1[H_2] + K_{2a}[O_a] + K_{2b}[O_b]\} - [Rh]_T = 0 \tag{12}$$

which is a non-linear algebraic equation that governs the concentration of the species AS to be used in the rate equations described by Eqs. (8) and (9). It should be noted that if $[AS]/K_0 \ll 1$, model M2 reduces to model M1. However, if $[AS]/K_0 \gg 1$ the hydrogenation rate is half-order with respect to the catalyst concentration $[Rh]_T$.

3.4.3. Derivation of model M3

In this model it is assumed that the species AS undergoes a second dissociation yielding the putative species AS_2, which could contribute to the catalytic process according to the following sequence of reactions:

$$AS + S \leftrightarrow AS_2 + L \quad K'_0\ (k'_0 \text{ and } k'_{-0}) \tag{13}$$

$$AS_2 + H_2 \leftrightarrow AS_2H_2 \quad K'_1\ (k'_1 \text{ and } k'_{-1}) \tag{14}$$

$$AS_2 + O_a \leftrightarrow AS_2O_a \quad K'_{2a}\ (k'_{2a} \text{ and } k'_{-2a}) \tag{15}$$

$$AS_2 + O_b \leftrightarrow AS_2O_b \quad K'_{2b}\ (k'_{2b} \text{ and } k'_{-2b}) \tag{16}$$

$$AS_2H_2 + O_a \rightarrow AS_2 + P_a \quad k'_{3a} \tag{17}$$

$$AS_2O_a + H_2 \rightarrow AS_2 + P_a \quad k'_{4a} \tag{18}$$

$$AS_2H_2 + O_b \rightarrow AS_2 + P_b \quad k'_{3b} \tag{19}$$

$$AS_2O_b + H_2 \rightarrow AS_2 + P_b \quad k'_{4b} \tag{20}$$

Adding these steps to those described by Eqs. (1)–(7) and (11), and solving for the simplifying assumptions results in the final rate equations:

$$R_a = \{k_{3a}K_1(1 + \hat{k}_{4a}\hat{K}_{2a})[AS] + k'_{3a}K'_1(1 + \hat{k}'_{4a}\hat{K}'_{2a}) \times [AS_2]\}[H_2][O_a] \tag{21}$$

$$R_b = \{k_{3b}K_1(1 + \hat{k}_{4b}\hat{K}_{2b})[AS] + k'_{3b}K'_1(1 + \hat{k}'_{4b}\hat{K}'_{2b}) \times [AS_2]\}[H_2][O_b] \tag{22}$$

where $\hat{k}'_{4a} = k'_{4a}/k'_{3a}$, $\hat{K}'_{2a} = K'_{2a}/K'_1$, $\hat{k}'_{4b} = k'_{4b}/k'_{3b}$ and $\hat{K}'_{2b} = K'_{2b}/K'_1$, Eqs. (21) and (22) being subjected to the following system of non-linear equations arising from the rhodium and phosphine balances

$$[AS]\left\{1 + \frac{[AS]}{K_0}\right\} \times \{1 + K_1[H_2] + K_{2a}[O_a] + K_{2b}[O_b]\} + [AS_2]\left\{1 + \frac{2[AS]}{K_0}\right\} \times \{1 + K'_1[H_2] + K'_{2a}[O_a] + K'_{2b}[O_b]\} - [Rh]_T = 0 \tag{23}$$

$$2[AS_2]^2 \times \{1 + K'_1[H_2] + K'_{2a}[O_a] + K'_{2b}[O_b]\} + [AS][AS_2] \times \left\{1 + K_1[H_2] + K_{2a}[O_a] + K_{2b}[O_b]\right\} - K'_0[AS] = 0 \tag{24}$$

which has to be solved for [AS] and [AS_2].

3.5. Parameter estimation procedure

The concentration [AS] in Eq. (12) of model M2 was found as real zero of a real function using Müller's method [12]. The system of non-linear equations governing [AS] and [AS_2] in model M3 was solved using a modified Powell hybrid algorithm and a finite-difference approximation to the Jacobian [13]. The numerical integration of the R_a and R_b rate equations was performed using a Runge-Kutta (2, 3) pair method [14]. The residual sum of squares was minimized using a modified Levenberg–Marquardt algorithm combined with an active strategy to solve non-linear least squares problems [15].

The optimization of the model parameters was achieved by fitting the experimental data in both time and temperature domains. A first optimization was performed at the reference temperature of 313 K, followed by a second optimization in the temperature domain. The temperature dependence of kinetic rate and equilibrium constants was assumed to obey the Arrhenius law

$$k(T) = k(T_r)\exp\left(-\frac{E}{RT'}\right) \tag{25}$$

and the Van't Hoff law

$$K(T) = K(T_r)\exp\left(-\frac{\Delta H}{RT'}\right) \tag{26}$$

respectively, where T' is given by

$$\frac{1}{T'} = \frac{1}{T} - \frac{1}{T_r} \tag{27}$$

and T_r is the reference temperature.

Concerning the significance of the estimated model parameters, the individual 95% confidence intervals were calculated. The selection of the most adequate model was performed using Fisher's test [16,17]

$$F_{calc} = \frac{\sum_{h=1}^{\upsilon}\sum_{k=1}^{\upsilon}\sigma^{hk}\sum_{i=1}^{n}C_{calc,ih}C_{calc,ik}/p}{\sum_{h=1}^{\upsilon}\sum_{k=1}^{\upsilon}\sigma^{hk}\sum_{i=1}^{n}(C_{obs,ih} - C_{calc,ih}) \times (C_{obs,ik} - C_{calc,ik})/(n\upsilon - p)}$$

where $C_{obs,ij}$ and $C_{cal,ij}$ are the observed and calculated concentrations values for the ith compound of the jth data point, respectively; σ^{hk} the elements of the inverse of the error covariance matrix ($\upsilon \times \upsilon$), n the number of experimental data per compound, υ the number of compounds and p the number of adjusted parameters of the model.

The regression was considered to be meaningful if the calculated F_c value exceeds the corresponding tabulated F-value, and the highest F_{calc} value was taken as indicative of the best possible regression. The adequacy of the fitting was also checked examining the residual sum of square (SSQ) and the residuals plots.

3.6. Results from parameter estimation

For parameter estimation purposes, avermectin and ivermectin (with series a and b resolution) concentrations versus time data from 1136 observations were used. After estimation of model parameters at the reference temperature, the data at all temperatures were simultaneously fitted by means of reparameterization given by Eqs. (25)–(27). Estimates were systematically searched from different sets of preliminary parameter values to find parameters that are physically meaningful. A reduction of the parameters in models M1–M3 was possible from an examination of the role of the relative parameters denoted by $\hat{k}_{4i}$ and $\hat{k}'_{4i}$ (i = a or

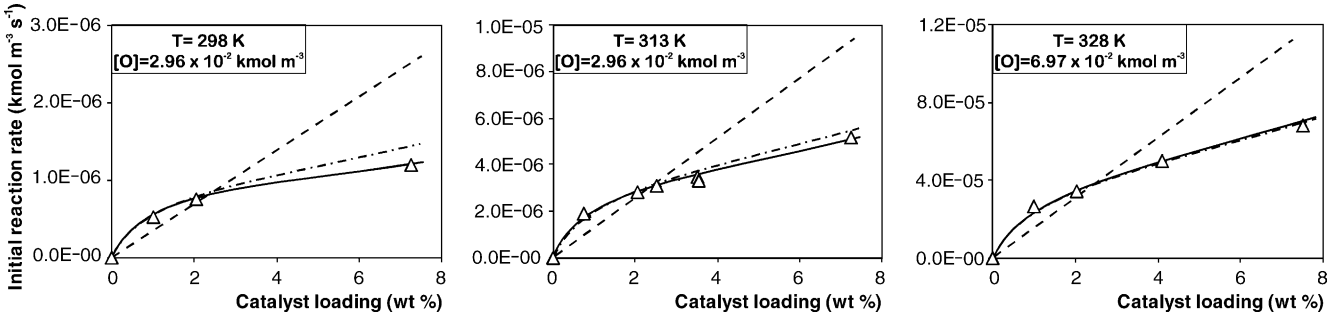

Fig. 7. Experimental and predicted initial reaction rates vs. the catalyst loading, at each temperature (298, 313 and 328 K). (Δ) experimental; (- - -) model M1; (· ·· ··) model M2; (—) model M3.

b). Their values were found to be much smaller than 1 for all three models. This finding confirms that the hydrogenation by route involving species $[RhCl(PPh_3)_2O]$ is negligible, as outlined above. The relative parameters were subsequently eliminated.

Differences between models M1–M3 are observed from the overall fit. Experimental and predicted initial reaction rates versus the catalyst loading are shown in Fig. 7. A simple visual inspection reveals that model M1 is significantly more inaccurate than the other two models, which appear to be almost indistinguishable. Also, large deviations between experimental and predicted composition profiles in the time domain are apparent at low and high catalyst loading for model M1, as depicted in Fig. 8 (only series B_{1a} is shown). Instead models M2 and M3 are able to describe the experimental data reasonably well in whole range of catalyst loading. Model M3 seems to give a slightly better description into the whole range of catalyst loading, but this could be mainly attributed to the great flexibility arising from their structure having twelve (model M3) instead of six (model M2) parameters. Residuals in the conversion domain at 313 K are shown in Fig. 9. The non-uniform and broad bands obtained for model M1 confirm the inadequacy of this model, whereas the narrow bands and the random scattering of errors for models M2 and M3 show the parity between them.

A better criterion for model comparison is given by the statistical analysis of the adequacy or lack of fit of the models. Table 1 summarizes the SSQ and F_{calc} values of the non-linear regression analysis for the three rival models at constant temperature (313 K). Model M1 exhibits the lowest F_{calc} value, which indicates the worst quality of the description of our experimental data. Although no significant differences between the models M2 and M3 arise from the SSQ values, both models are quite distinct from the statistical point of view. According to the F_{calc} values, the model M2 is the best candidate since it provides practically the same description of the concentration profiles with a smaller number of parameters. An optimization in the whole temperature range restricted also the possible best kinetic description to model M2, as revealed by the F_{calc} values in Table 2. These results suggest that a mechanism of reaction featuring simple dissociation of the catalyst precursor and the olefin coordination step as rate-determining is fair enough to describe the hydrogenation of this macrocyclic lactone.

The calculated model parameters and confidence intervals for model M2 are shown in Table 3. The equilibrium constant for the dissociation of $RhCl(Ph_3P)_3$ in toluene solution of avermectins was found to be $(2.02 \pm 0.12) \times 10^{-6}$ kmol m^{-3} at 313 K. This value of K_0, although quantitatively rather smaller than expected since $K_0 = (1.4 \pm 0.4) \times 10^{-4}$ kmol m^{-3} in benzene solution at 298 K [18], is sufficiently small to support the same conclusion derived from other olefin hydrogenation reactions catalysed with this catalyst, namely that the dissociation of $RhCl(Ph_3P)_3$ is not extensive. Moreover, the K_{2a}/K_1

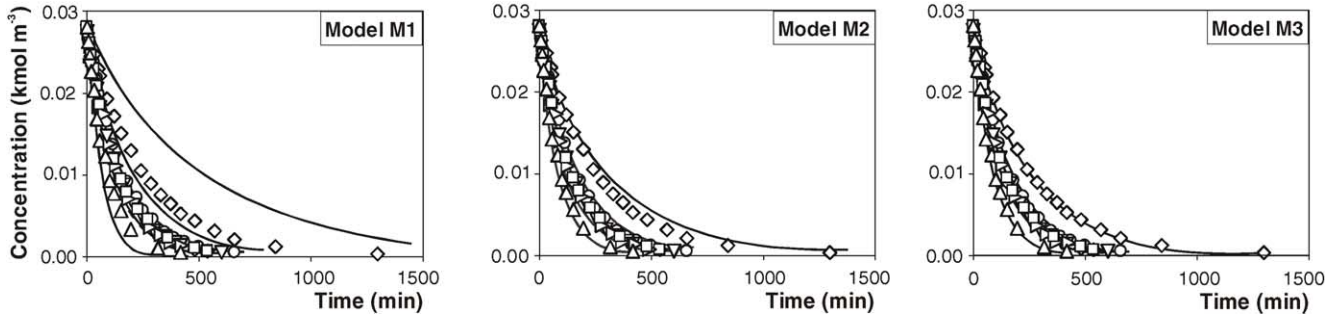

Fig. 8. Experimental and predicted composition profiles in the time domain, at 313 K and 275.7 kN m^{-2}, in the whole range of catalyst loading (wt.%): (◇) 0.75; (○) 2.05; (▽) 2.53; (▷) 3.52; (□) 3.55; (△) 7.25. Full-line: model predictions.

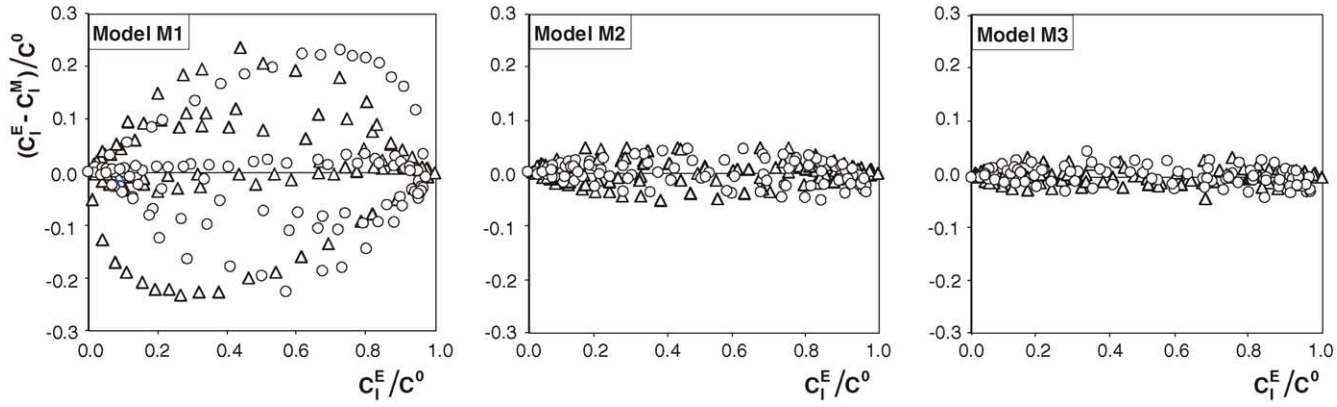

Fig. 9. Residuals between the predictions of the models and the experimental data in the time domain, at 313 K and 275.7 kN m^{-2}. (△) avermectin; (○) ivermectin.

Table 1
Residual sum of squares (SSQ) and F-test (F_{calc}) values for the kinetic models and the set of experimental data at 313 K and 275.7 kNm^{-2}, in the whole catalyst loading range[a]

Model	Number of parameters	SSQ	F_{calc}
M1	5	1.48×10^{-3}	410.53
M2	6	9.14×10^{-5}	5516.68
M3	12	1.46×10^{-4}	1622.31

[a] Number of experimental data = 424.

Table 2
Residual sum of squares (SSQ) and F-test (F_{calc}) values for the kinetic models and the set of experimental data in the whole temperature and catalyst loading ranges[a]

Model	Number of parameters	SSQ	F_{calc}
M1	5	7.05×10^{-3}	1012.66
M2	6	6.36×10^{-4}	9429.16
M3	12	8.08×10^{-4}	3613.84

[a] Number of experimental data = 1136.

ratio was estimated to be 6.15×10^{-4}, which is consistent with a prevalent ability of species [RhCl(Ph$_3$P)$_2$(S)] to activate molecular hydrogen yielding species [RhCl(PPh$_3$)$_2$H$_2$(S)] more than the olefin to give species [RhCl(PPh$_3$)$_2$O]. This value of K_{2a}/K_1 is fairly smaller than those reported for not too large olefins, which can be attributed to the steric hindrance of this macrocyclic lactone. The observed half-order dependence of the catalyst loading on the hydrogenation rate also follows from the [AS]/K_0 ratio values, which were found to be in the 5–20 range. Since [AS]/$K_0 > 1$ in Eq. (12), the second-order dependence of [AS] prevails on the first-order one and determines the observed half-order dependence on the catalyst loading. In addition, the [AS]/K_0 ratio values reveal that the catalyst precursor only dissociates to the extent of 4.7–16.7% for catalyst loading ranging from 7.25 to 0.75 wt.%, respectively.

The values of the kinetic constants k_{3a} and k_{3b} were found to be only about 20–40% smaller than those reported for the cyclohexene hydrogenation [2], which confirms the good intrinsic reactivity of the 22–23 olefinic linkage of avermectins B$_{1a}$ and B$_{1b}$ spite of their large molecular size. The heat of dissociation of the catalyst precursor was found to be around 21 kJ mol^{-1}, and the values of ($-\Delta H$) evidence a favorable temperature effect on the formation of the dihydrido-complex relative to the other complexes. The activation energies of 78.94 and 82.78 kJ mol^{-1} were obtained for the rate-determining steps, which are in good agreement with those found for the homogeneous hydrogenation of olefins catalyzed with rhodium complexes.

4. Conclusions

It was shown that the purification of commercial avermectins and the in situ preconditioning of the reaction medium following the developed experimental procedures are important prerequisites for obtaining reliable data to study the kinetics of the hydrogenation of avermectins B$_{1a}$ and B$_{1b}$ catalyzed by RhCl(Ph$_3$P)$_3$ complexes. From the observed dependence of the hydrogenation rates on the catalyst, avermectins, and hydrogen concentrations, it was possible to propose plausible reaction schemes based on the

Table 3
Fitted parameter values for the kinetic model M2 with 95% confidence limits

K_0 (kmol m^{-3})	$(2.02 \pm 0.12) \times 10^{-6}$	$-\Delta H_0$ (kJ mol^{-1})	21.08 ± 0.03
K_1 (kmol^{-1} m^3)	$(1.74 \pm 0.06) \times 10^{2}$	$-\Delta H_1$ (kJ mol^{-1})	4.22 ± 0.10
K_{2a} (kmol^{-1} m^3)	$(1.07 \pm 0.02) \times 10^{-1}$	$-\Delta H_{2a}$ (kJ mol^{-1})	20.53 ± 0.03
K_{2b} (kmol^{-1} m^3)	$(1.05 \pm 0.10) \times 10^{-1}$	$-\Delta H_{2b}$ (kJ mol^{-1})	20.88 ± 0.01
k_{3a} (kmol^{-1} m^3 s^{-1})	$(3.60 \pm 0.18) \times 10^{0}$	E_{3a} (kJ mol^{-1})	78.94 ± 0.14
k_{3b} (kmol^{-1} m^3 s^{-1})	$(2.70 \pm 0.20) \times 10^{0}$	E_{3b} (kJ mol^{-1})	82.78 ± 0.14

main steps suggested by Wilkinson for simple olefin hydrogenation. A statistical analysis of regression allowed the indubitable exclusion of the kinetic model based on the complete dissociation of the catalyst precursor, since unacceptable SSQ and F_{calc} values arose from its inadequacy to describe the observed half-order reaction with respect to the catalyst loading. However, it was possible to fit reasonably well the experimental data considering mechanisms of reaction featuring no extensive simple (first) and double (first and second) dissociation of the catalyst precursor, and reaction pathway following the hydride route with the olefin coordination step as rate-determining. Although according to the SSQ values it was difficult to distinguish between the models having simple and double dissociation of the catalyst precursor, both models were quite distinct from the statistical point of view. According to the F_{calc} values, it was emphasized that the model with only simple dissociation is statistically the best candidate since it provides practically the same quality of description of our experimental data with a smaller number of parameters. Thus we conclude that this model proved to be the simplest one for the description of the hydrogenation of avermectins B_{1a} and B_{1b} to ivermectin in toluene solution, under conditions of 298–328 K at 275.7 kN m^{-2}, using catalyst loading in the range of 0.75–7.25 wt.% with respect to the avermectins.

Acknowledgments

The authors wish to express their gratitude to the Agencia Nacional de Promoción Científica y Tecnológica (ANPCyT), to Consejo Nacional de Investigaciones Científicas y Técnicas (CONICET), and to Universidad Nacional del Litoral (UNL) of Argentina, for the financial support granted to this contribution. Thanks are given to Rubén Malizia for his valuable help in the development of some of the practical aspects of the hydrogenation technique.

Appendix A. Gas–liquid mass transfer effects

Gas–liquid mass transfer resistance values are generally restricted to the particular stirred reactor configuration. Moreover, the presence of the bisoleandrosyloxy substituent attached to the C13 of the macrocycle lactone confers an amphiphatic structure to the avermectins and, therefore, some surface activity that could promote the formation of the interface area. Consequently, the experimental determination of this resistance is desirable upon any estimation based on correlations.

The experimental set-up is able to provide precise experimental determination of the gas–liquid mass transfer resistance from data of initial hydrogenation rates at different catalyst loadings [7]. Since the reaction rate is half-order and first-order with respect to the catalyst loading and substrate concentration, respectively (see Figs. 4 and 5), and lower than pseudo-first order with respect to the hydrogen concentration (see Fig. 6), hydrogen transport and reaction rate equations can be combined in a single rate equation as follows:

$$\frac{[H_2^*]}{R_H^0} = \frac{1}{k_b a_b} + \frac{(1 + K_1[H_2^0])^{0.5}}{k[O^0]} \frac{1}{[Rh]_T^{0.5}}$$

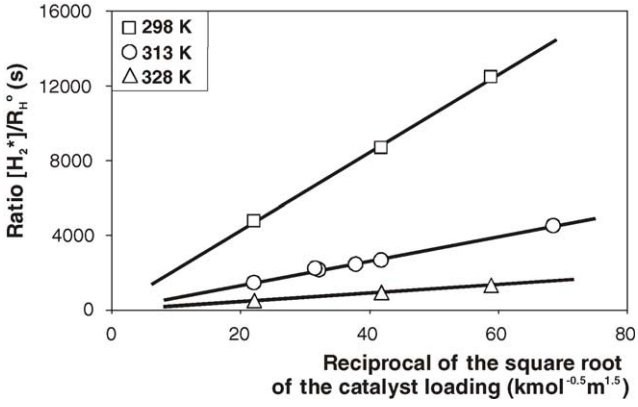

Fig. A.1. Determination of the gas–liquid resistance for the hydrogen transfer at different temperatures. Hydrogen pressure of 275.7 kN m^{-2}, and stirring rate of 250 rpm.

Table A.1
Results for the estimation of the gas–liquid mass transfer resistance at the different catalyst loading and temperatures, avermectin concentration of 2.96×10^{-2} kmol m^{-3}, hydrogen pressure of 275.7 kN m^{-2}, and stirring rate of 250 rpm

$[Rh]_T$ (%)	T (K)	R_b (s)	Initial R_c (s)	Minimum R_b/R_c	$k_b a_b \times 10^2$ (s^{-1})	Maximum $1 - [H_2]/[H_2^*]$ (%)
1.03	298	64.63	12326.00	190.72	1.54	0.52
2.05	298	64.63	8747.49	135.35	1.54	0.75
7.26	298	64.63	4645.79	71.88	1.54	1.36
0.76	313	45.53	4445.97	96.65	2.19	1.01
2.05	313	45.53	2709.06	59.50	2.19	1.72
2.53	313	45.53	2462.78	54.09	2.19	1.87
3.52	313	45.53	2086.88	45.83	2.19	2.12
3.55	313	45.53	2054.48	45.12	2.19	2.03
7.26	313	45.53	1438.78	31.60	2.19	3.15
1.03	328	35.84	1285.79	35.87	2.79	2.70
2.05	328	35.84	912.49	25.46	2.79	3.80
7.26	328	35.84	484.63	13.52	2.79	6.82

where $k_b a_b$ is the gas–liquid overall mass transfer coefficient, and k an apparent rate constant. The first term is the gas–liquid mass transfer resistance (R_b), and the second term is the initial chemical reaction resistance (R_c). For hydrogenation runs carried out at constant initial concentrations of both substrate and hydrogen, a plot of $[H_2^*]/[R_H^0]$ versus $1/[Rh]_T^{0.5}$ should be a straight line with an intercept of $1/k_b a_b$.

The experimental procedure guarantees the same initial substrate and hydrogen concentrations, and the absence of induction times. The initial reaction rates were determined by fitting the substrate concentration versus time plots with an exponential function, and calculating the slope at time equal to zero. The values of the concentration of the hydrogen dissolved in the reaction medium were calculated based on the hydrogen solubility in toluene [11]. Thus, the values of $[H_2^*]/[R_H^0]$ were plotted against the reciprocal of the square root of the catalyst loading. Fig. A.1 shows a good straight line correlation at 298, 313, and 328 K. Table A.1 summarizes the values of R_b and R_c resistances. For our experimental conditions, it was found that $R_c \gg 10R_b$, i.e. the chemical reaction resistance is prevalent. The values of the gas–liquid overall mass transfer coefficient were found to be 1.54×10^{-2}, 2.19×10^{-2}, and $2.79 \times 10^{-2}\ s^{-1}$, at 298, 313, and 328 K, respectively. Therefore, the values of the ratio between the highest initial reaction rate and the maximum mass transfer rate of hydrogen, i.e., $1 - [H_2]/[H_2^*]$, were found to be in the range of 0.005–0.014, 0.010–0.031, and 0.027–0.068, at 298, 313, and 328 K, respectively. Thus, only the experimental data for the initial step of the hydrogenation run carried out under the most demanding conditions (catalyst loading of 7.26 wt.%, at 328 K) are moderately affected by the gas absorption resistance. However, this undesirable effect is practically negligible in all other hydrogenation runs because the values of $1 - [H_2]/[H_2^*]$ are less than 0.038.

References

[1] J. Chabala, H. Mrozik, R. Tolman, P. Eskola, A. Lusi, L. Peterson, M. Woods, M. Fisher, W. Campbell, J. Egerton, D. Ostlind, J. Med. Chem. 23 (1980) 1134.
[2] J. Osborn, F. Jardine, J. Young, G. Wilkinson, J. Chem. Soc. A (1966) 1711.
[3] J.C. Chabala, M.H. Fisher, USP 4,199,569 (1978), to Merck & Co.
[4] D. Arlt, G. Bonse, USP 5,656,748 (1997), to Bayer.
[5] D. Arlt, G. Bonse, USP 6,072,052 (2000), to Bayer.
[6] L. Sogli, D. Siviero, A. Rossi, D. Terrasar, et al., WO 98/38201 (1998), to Alfonso Giambrocono et al.
[7] R. Grau, A. Cassano, M. Baltanás, Ind. Eng. Chem. Res. 26 (1987) 18.
[8] Ch. O'Connor, G. Wilkinson, J. Chem. Soc. A (1968) 2665.
[9] Ch. O'Connor, G. Wilkinson, Tetrahedron Lett. 18 (1969) 1375.
[10] T.-F. Mao, G.L. Rempel, J. Mol. Catal. A: Chem. 135 (1998) 121.
[11] J. Connoluy, J. Chem. Phys. 36 (1962) 2897.
[12] D.E. Müller, Math. Tables Aids Comput. 10 (1956) 208.
[13] J. More, B. Garbow, K. Hillstrom, User guide for MINPACK-1, Argonne National Labs Report ANL-80, 74, Argonne, Illinois, 1980.
[14] R.W. Brankin, I. Gladwell, L.F. Shampine, RKSUITE: A Suite of Runge Kutta Codes for the Initial Value Problem for ODES, Softreport 91–1, Mathematics Department, Southern Methodist University, Dallas, Texas, 1991.
[15] D.W. Marquardt, J. Soc. Ind. Appl. Math. 11 (1963) 431.
[16] G.F. Froment, L.H. Hosten, in: J.R. Anderson, M. Boudart (Eds.), Catalysis Science and Technology, vol. 2, Springer-Verlag, Berlin, 1981, p. 97.
[17] G.F. Froment, K.B. Bischoff (Eds.), Chemical Reactor Analysis and Design, 2nd ed. Wiley, New York, 1990.
[18] H. Arai, J. Halpern, Chem. Commun. (1971) 1571.